DOI: 10.1534/genetics.107.081638

A Screen for Modifiers of Hedgehog Signaling in *Drosophila melanogaster* Identifies *swm* and *mts*

David J. Casso,* Songmei Liu,* D. David Iwaki,* Stacey K. Ogden† and Thomas B. Kornberg*,[1]

**Department of Biochemistry and Biophysics, University of California, San Francisco, California 94158-2711 and †Department of Pharmacology and Toxicology, Dartmouth Medical School, Hanover, New Hampshire 03755*

Manuscript received September 6, 2007
Accepted for publication December 21, 2007

ABSTRACT

Signaling by Hedgehog (Hh) proteins shapes most tissues and organs in both vertebrates and invertebrates, and its misregulation has been implicated in many human diseases. Although components of the signaling pathway have been identified, key aspects of the signaling mechanism and downstream targets remain to be elucidated. We performed an enhancer/suppressor screen in Drosophila to identify novel components of the pathway and identified 26 autosomal regions that modify a phenotypic readout of Hh signaling. Three of the regions include genes that contribute constituents to the pathway—*patched*, *engrailed*, and *hh*. One of the other regions includes the gene *microtubule star* (*mts*) that encodes a subunit of protein phosphatase 2A. We show that *mts* is necessary for full activation of Hh signaling. A second region includes the gene *second mitotic wave missing* (*swm*). *swm* is recessive lethal and is predicted to encode an evolutionarily conserved protein with RNA binding and Zn^{+} finger domains. Characterization of newly isolated alleles indicates that *swm* is a negative regulator of Hh signaling and is essential for cell polarity.

HH signaling is essential to the development of many tissues and organs in both vertebrates and invertebrates, and it has important medical implications. *hh* was first identified as a gene that is required for segmentation of the Drosophila embryo (Nusslein-Volhard and Wieschaus 1980); subsequent studies have established roles at all developmental stages in a variety of cell types. When signaling is reduced in human, sheep, fish, and mouse embryos, severe holoprosencephaly and cyclopia result (Belloni *et al.* 1996; Chiang *et al.* 1996; Roessler *et al.* 1996; Schier *et al.* 1997). Increased signaling in human adults can lead to cancers of the skin, cerebellum, muscle, digestive tract, pancreas, and prostate (reviewed in Pasca Di Magliano and Hebrok 2003). Hh signaling is complex, and a complete understanding of Hh signaling will encompass the mechanism and regulation of active Hh protein production, its release from producing cells, its transit to target cells, the mechanism that senses its presence in target cells, and the output of the pathway on patterning and growth.

Synthesis of the mature Hh peptide involves multiple steps, including cleavage of a signal sequence from an inactive precursor, autoproteolysis, N-terminal palmitoylation, and C-terminal cholesteroylation (Porter *et al.* 1996; Pepinsky *et al.* 1998). The N-terminal lipid is essential for Hh activity (Chamoun *et al.* 2001; Lee and Treisman 2001; Micchelli *et al.* 2002). The C-terminal cholesterol is needed to generate the normal distribution of transported protein (Porter *et al.* 1996; Gallet *et al.* 2003; Dawber *et al.* 2005; Callejo *et al.* 2006; Gallet *et al.* 2006). Release of lipid-modified Hh requires the Dispatched protein (Burke *et al.* 1999), but how Dispatched interacts with and affects Hh awaits clarification. Movement of Hh away from producing cells may involve interactions with proteoglycans (reviewed in Eaton 2006) and may require assembly into a multimer form (Zeng *et al.* 2001; Chen *et al.* 2004; Feng *et al.* 2004; Gallet *et al.* 2006;).

In target cells, several membrane proteins contribute to the recognition of Hh— Patched (Ptc), Interference Hedgehog (Ihog), Brother of Ihog, and Smoothened (Smo) (Hooper 1994; Chen and Struhl 1996; Quirk *et al.* 1997; Yao *et al.* 2006). In the absence of Hh, Ptc inhibits Smo-dependent signal transduction. In the presence of Hh, Smo accumulates at the cell surface (Zhang *et al.* 2001, 2004; Apionishev *et al.* 2005; Lu *et al.* 2006) and binds through its intracellular C-terminal tail to a Hh signaling complex. Other constituents of this complex include the kinase Fused, (Fu), the kinesin-related motor protein Costal2 (Cos2), Suppressor of Fused (SuFu), and the Zn+ finger transcription factor Cubitus interruptus (Ci). It is thought that Hh binding to Ptc alters the composition and localization of this and derivative protein complexes in ways that are sensitive to Hh concentration (reviewed in Hooper and Scott 2005; Ogden *et al.* 2006). Although we lack a complete under-

Sequence data from this article have been deposited with the EMBL/GenBank Data Libraries under accession nos. EF601876 and EF601878.

[1]*Corresponding author:* Department of Biochemistry and Biophysics, University of California, San Francisco, CA 94143-2711.
E-mail: tkornberg@biochem.ucsf.edu

standing of how the presence of Hh at the cell surface leads to changes in expression of target genes, we know that the responses of Smo, Cos2, and Ci to Hh are mediated, in part, by phosphorylation. Smo requires several phosphorylation sites in its C-terminal tail for activity (Chen *et al.* 1998; Price and Kalderon 2002; Jia *et al.* 2004; Collins and Cohen 2005), phosphorylation of Cos2 by Fu promotes cell surface accumulation and stabilization of Smo (Nybakken *et al.* 2002; Lu *et al.* 2006), and Ci phosphorylation is required for conversion to either its repressor or activator forms (Chen *et al.* 1998; Price and Kalderon 2002).

Hh signaling is arguably best understood in the context of its roles in the imaginal discs where it governs patterning and cell growth. In the eye imaginal discs, for instance, Hh signals regulate cell proliferation directly in the receiving cells by inducing Cyclin D and Cyclin E (Duman-Scheel *et al.* 2002). In the wing disc, *hh* is positively regulated by Engrailed (En), and both *hh* and *en* are expressed by all P-compartment cells (Tabata *et al.* 1992). Hh protein moves across the A/P compartment border (Tabata and Kornberg 1994) to activate such genes as *ptc* and *decapentaplegic* (*dpp*) in A cells, creating a developmental organizer among the Anterior Hh-responding cells adjacent to the compartment border (Tabata *et al.* 1995; Zecca *et al.* 1995). Hh signals regulate cell proliferation in the receiving cells by inducing Dpp, the predominant mitogen for this tissue. In addition, Hh itself has a mitogenic role independent of Dpp in the wing cells between veins 3 and 4 (Mullor *et al.* 1997; Strigini and Cohen 1997). The sensitivity of these cells to Hh levels is manifested by an expansion of the intervein region when signaling increases and a corresponding reduction when it decreases. We have tapped this sensitivity to identify novel components of the Hh signaling pathway with a genetic screen.

Several types of screens for Hh pathway components have been carried out previously. Published genetic screens were based on the wing phenotypes of known pathway mutants (Vegh and Basler 2003), on suppression of a gain of function *hh* mutant (Haines and van den Heuvel 2000), or on enhancement or suppression of a partial loss-of-function phenotype generated by a dominant negative form of Smo (Collins and Cohen 2005). These screens identified a new class of *ptc* mutants (Vegh and Basler 2003), mutations that affect Hh stability (Haines and van den Heuvel 2000), and implicated the translation factors eRF1 and elF1A and the kinesin-like protein Pavarotti in the Hh response (Collins and Cohen 2005). Genomewide RNA interference (RNAi) assays in cultured cells identified many functions that contribute to Hh responses (Lum *et al.* 2003; Nybakken *et al.* 2005). These include components of the ribosome, the vesicular transport pathway, the RNA splicing and transport pathways, and several protein kinases (Nybakken *et al.* 2005), as well as Hh-binding proteins such as Ihog (Lum *et al.* 2003; Yao *et al.* 2006).

In this report, we describe a deficiency screen for genomic regions that enhance or suppress a smo partial loss-of-function wing vein phenotype. Twenty-six regions were identified that scored in this screen; twenty-two of these do not contain genes that encode known Hh pathway components. We report on the characterization two genes located in these regions: *microtubule star* (*mts*; Snaith *et al.* 1996), which positively regulates Hh signaling and whose loss of function enhances the smo knockdown phenotype; and *second mitotic wave missing* (*swm*; Gay and Contamine 1993), which negatively regulates Hh signaling and whose loss of function suppresses the smo knockdown phenotype.

MATERIALS AND METHODS

Drosophila stocks and culture: Deficiency kit collections of stocks carrying deletions for chromosomes 2 and 3 were obtained from the Bloomington Drosophila Stock Center (Bloomington, IN). These deletions are estimated to cumulatively delete 92–95% of the euchromatin (flystocks.bio.indiana.edu). Stocks carrying mutations in candidate genes were obtained from individual labs and from the Bloomington and Szeged Stock Centers. Stocks expressing RNAi's of candidate genes were generously provided by R. Ueda and K. Fujitani (National Institute of Genetics, Mishima, Japan). Flies were cultured on standard cornmeal/molasses medium at 25°; crosses with *smo RNAi* were carried out at 29°.

Molecular cloning and sequence analysis: PCR products were generated using Vent DNA Polymerase (New England Biolabs, Beverly, MA), subcloned into *pCR2.1-TOPO* (Invitrogen, Carlsbad, CA), and sequenced. A *smo* hairpin RNAi in "tail to tail" orientation was cloned into the *GAL4*-inducible RNAi vector *pWIZ* (Lee and Carthew 2003) to create *pWIZ-smo* (Ogden *et al.* 2006). To generate *pUAS-swm*, a *swm* cDNA was amplified (primer pair: TTTCTCGAGATGATTCTGGA GAATTCGGACAAGC and TTTTCTAGATCAACGACGCCAG GAGCGATCCTCG) and the product was subcloned into *pUAST* (Brand and Perrimon 1993). To generate *GFP-Swm*, *GFPS65T* was amplified (primer pair: TTTCTCGAGATGATT CTGGAGAATTCGGACAAGC and TTTCTCGAGTTTGTATA GTTCATCCATGCC), a *swm* (CG10084) cDNA was amplified (primer pair: TTTCTCGAGATGATTCTGGAGAATTCGGAC AAGC and CGAGGATCGCTCCTGGCGTCGTTGATCTAGA AAA), and the products were ligated together after *Xho*I digestion. The resulting fusion protein was subcloned into *pUAST* after *Xba*I digestion.

Protein sequence was analyzed for motifs with InterProScan (http://www.ebi.ac.uk/InterProScan; Apweiler *et al.* 2001) and PredictNLS (http://cubic.bioc.columbia.edu/predictNLS; Cokol *et al.* 2000).

Cell and tissue staining: Drosophila S2 cells were cultured in Shields and Sang M3 media (Sigma, St. Louis) supplemented with 10% heat-inactivated fetal bovine serum. To determine the subcellular localization of GFP-Swm, S2 cells were cotransfected with *pA5c-GAL4* (Ramirez-Weber *et al.* 2000) and *pUAS-GFP-swm* using Effectene (QIAGEN, Valencia, CA). After 48 hr, cells were transferred to Lab-Tek Permanox chamber slides (Nagle Nunc International, Rochester, NY) coated with concanavalin A (Sigma-Aldrich, St. Louis) for 20 min prior to examination using a 100× objective. Imaginal discs from wandering third instar larvae were fixed in PBS containing 4% formaldehyde for 20 min, and stained overnight in PBS containing 5% normal donkey serum and 0.3%

Triton X-100 with affinity-purified monoclonal mouse anti-Ptc antisera (1:50; Capdevila *et al.* 1994), or rat monoclonal anti-Ci antisera (1:2000; Motzny and Holmgren 1995), followed by detection with Alexaflour-488 or -555 conjugated secondary antibodies (Invitrogen, Carlsbad, CA). Wings were mounted in Euparol. To estimate cell size in the wing blade, the intervein region between veins 4 and 5 of 11 wings of each genotype was photographed, and the number of wing hairs from equal-sized regions was counted.

***smo* interaction screen:** A y^1 *w*; ptcGAL4 P{WIZ-smo}*^{2B} chromosome which causes a partial fusion of longitudinal wing veins 3 and 4 was screened for enhancement or suppression when crossed to deficiency kits for chromosomes 2 and 3 (Bloomington Drosophila Stock Center). Chromosomes harboring deletions from deficiency kits were initially outcrossed into a y^- background and placed over a corresponding autosome marked with y^+: males carrying chromosome 2 deletions were crossed with stock B-1816 females (y^1 *w*^{1118}*; P{Car20y}*^{25F} *FRT40A*), and males with chromosome 3 deletions were crossed with B-16761 females (y^1 *w*^{67c23}*; P{EPgy2}CG17370*^{EY06831}). Males with third chromosome deletions balanced over *TM2* (*emc*^{2} *Ubx*^{130} *e*^{s}) were initially outcrossed to B-20124 females (y^1 *w*^{67c23}*; P{EPgy2}emc*^{EY01657}*/TM3, Sb*^{1} *Ser*^{1}). Phenotypically y^+ male progeny from these crosses carrying the deficiency over y^+ were then mated with y^1 *w*; ptcGAL4 P{WIZ-smo}*^{2B} females at 29°. (For deficiencies balanced over *TM2*, the y^+ emc$^+$ male progeny that carry deficiencies over the y^+ marked third chromosome were used.) Among the progeny of this second cross, y^+ control male flies were compared with their y^- siblings carrying the deletion chromosomes. In this way, each of the deficiency stocks was backcrossed once before testing its effects on the wing *smo RNAi* phenotype, and all of the crosses scored for enhancement/suppression had an internal sibling control. An example of this strategy for chromosome 2 is diagrammed below. Any deficiency chromosome which carried a y^+ marker was backcrossed initially to y^1, *w** females, male progeny were then crossed to y^1 *w*; ptcGAL4 P{WIZ-smo}*^{2B} females at 29°, and y^+ male progeny carry the deficiency were compared to their y^- control siblings. Deficiencies that scored as enhancers or suppressors were retested. Crossing scheme for enhancer/suppressor screen is as follows:

$$\frac{+}{Y};\ \frac{Df(2L)X}{CyO} \times y, w; P\{y^+\}$$

$$\downarrow$$

$$\frac{y, w}{Y};\ \frac{Df(2L)X}{P\{y^+\}} \times y, w;\ ptc\text{-}GAL4, WIZ\text{-}smo$$

$$\swarrow \qquad \searrow$$

$$\frac{y, w}{Y};\ \frac{Df(2L)X}{ptc\text{-}GAL4, WIZ\text{-}smo} \qquad \frac{y, w}{Y};\ \frac{P\{y^+\}}{ptc\text{-}GAL4, WIZ\text{-}smo}.$$

(experimental) (control)

Candidate *smo* modifier genes in regions that scored in the screen were tested with stocks carrying smaller deletions, *UAS-RNAi* lines, or extant alleles. RNAi lines were screened using both *ptcGAL4 P{WIZ-smo}* (in which *smo* activity is reduced in the Hh-receiving cells) and y^1 *w*; C765GAL4 UAS-smo*^{5A} (in which a dominant negative allele of *smo* is expressed in both anterior and posterior compartment cells, causing a reduction in wing size (Collins and Cohen 2005). Any mutant alleles, RNAi lines, or minimal deficiencies found to enhance or suppress both *smo RNAi* and *smo*^{5a} were then tested for nonspecific effects in a cross to y^1 *w*; P{GAL4-vg.M}*^{2} *pUAS-cutRNAi*^{1} (generously provided by Wesley Gruber and Yuh-Nun Jan), which produces a jagged wing-blade margin.

Isolation of *swm* alleles: Male flies (B-1646) *w*^{1118}*; P{white-un1}*^{30C} *FRT40A* were desiccated and starved at room temperature for 6 hr, followed by 24 hr with 7.5 mm 1,3-butadiene diepoxide (Sigma-Aldrich) in 1% sucrose (Reardon *et al.* 1987). As diagrammed below, treated flies were mated with y^1 *w*^{67c23}*; In(2LR)Gla wg*$^{Gla\text{-}1}$*/SM6a* females *en masse* for 3 days, after which the males were removed. Progeny carrying mutagenized second chromosomes balanced with *SM6a* were crossed to *swm*$^{37Dh\text{-}1}$*, pr*^{1} (Gay and Contamine 1993) balanced with *CyO-WeeP*, a GFP-tagged *CyO* balancer (Clyne *et al.* 2003). Non-complementing w$^+$, pr$^+$, and GFP$^+$ progeny were recovered and tested for complementation with *Df(2L) Exel8041*, which removes *swm* among ~40 genes in 37D7–37F2. To identify lesions in the *swm* gene from *swm* mutant stocks, the *swm* locus was amplified in two segments from genomic DNA essentially as described (Casso *et al.* 2005) using the following primer pairs: AAATCGCAGGAGCACAGTCG and TGCTGTCGTTAT GCCAGAAGACCT; and AACGAAACGAAAGGTGCCG and GGTAACACCGATAAAAAGTGGCG. Genomic DNA from *GFP*$^-$ larval progeny of *swm/ CyO*-GFP stocks was isolated and three independent PCR products were subcloned into pCR2.1-TOPO and sequenced. Crossing scheme for *swm* allele isolation is as follows:

$$w; *, p\{w^+\}, FRT^{40A}(iso) \times w; Gla/SM6a, pr$$

$$\downarrow$$

$$\frac{*, p\{w^+\}, FRT^{40A}}{SM6a,\ pr} \times \frac{swm^{DH1}, pr}{CyO, kr\text{-}GFP, pr}.$$

Wing analysis: Interactions with *hh*^{Mrt} were scored by classifying the severity of wing malformations with a system similar to that described by Felsenfeld and Kennison (1995). Class I, wild type; II, margin defects (*e.g.*, thickened margin), without any distortion of wing shape; III, anterior overgrowths, but without duplications or blistering; and IV, severe overgrowths which are rounded, have duplications, or show blistering. Approximately 100 wings from male flies were analyzed from each cross. The results of representative *hh*^{Mrt} crosses are presented in the text as percentages for each class.

To calculate the relative sizes of the regions between veins 3 and 4 in *swm*^{DH1}*/swm*^{F15} escaper and wild-type wings, wings were mounted in Euparol and photographed. Prints were cut between the alula and costa to remove the hinge, then along veins 3 and 4. The size of each region (anterior margin to vein 3, from vein 3 to vein 4, and from vein 4 to posterior margin) was measured by weighing the respective piece and normalizing it to the total size of the wing. In all cases of quantitation, errors indicate standard deviation.

Clonal analysis: Clones were induced with either a negative marking system (*hsflp, Ubi-GFP(S65T)nls*^{2L} *FRT40A*), or the positive MARCM system (Lee *et al.* 2000) using *y* w* hsFLP; tubP-GAL80*^{LL10} *FRT40A/CyO ActGFP*^{JMR1}*; tubP-GAL4*^{LL7}*, UAS-mCD8::GFP*^{LL6}*/TM6 Tb*^{1} (Bello *et al.* 2006). *M*$^+$ clones of *swm* in a *M/+* background were generated with *w*; M(2)24F*^{1} *P{piM}36F FRT40A*. Germline clones were generated by the FLP-DFS technique with the stock *P{ovoD1-18}*^{2La} *P{ovoD1-18}*^{2Lb} *FRT40A/CyO* (Chou and Perrimon 1992).

RESULTS

A screen for enhancers and suppressors of *smo* wing phenotype: The screen we carried out is based on comparisons of euploid and partially haploid flies that have

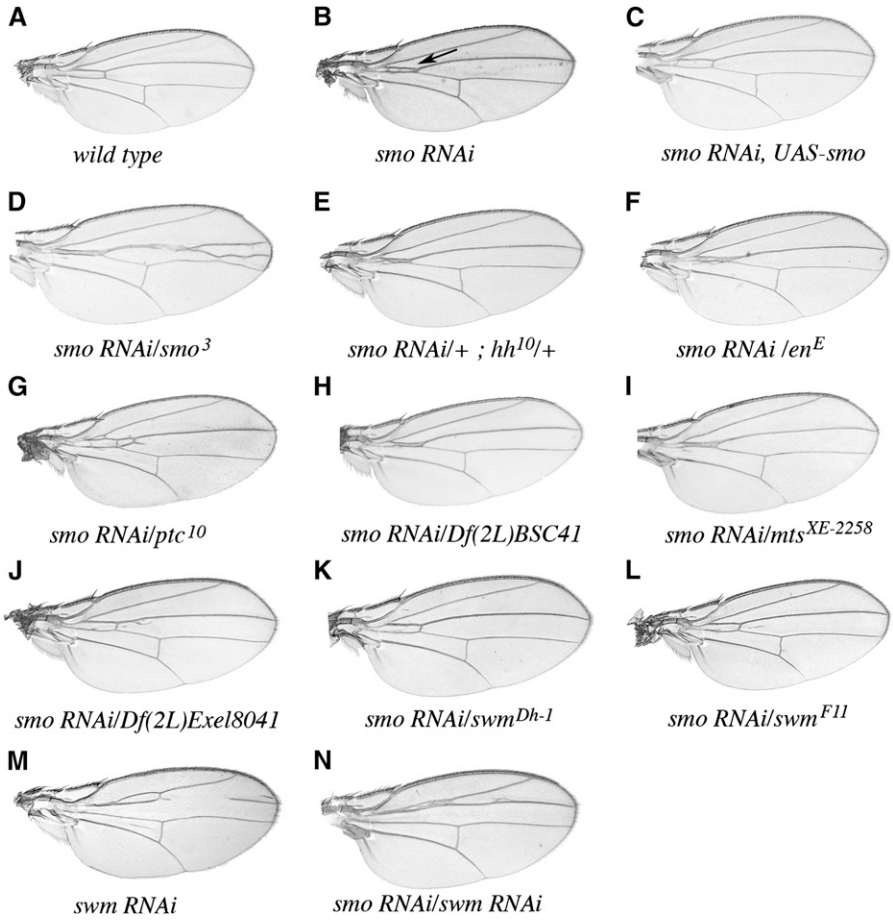

FIGURE 1.—*smo RNAi* in the adult wing. (A) wild type, (B) *ptcGAL4 WIZ-smo/+*, (C) *ptcGAL4 WIZ-smo/ UAS-smo*, (D) *ptcGAL4 WIZ-smo/smo*^{3}, (E) *ptcGAL4 WIZ-smo/+*, *hh*^{10}*/+*, (F) *ptcGAL4 WIZ-smo/en*^{E}, (G) *ptcGAL4 WIZ-smo/ptc*^{10}, (H) *ptcGAL4 WIZ-smo/Df(2L)BSC41*, (I) *ptcGAL4 WIZ-smo/mts*$^{XE-2258}$, (J) *ptcGAL4 WIZ-smo/Df(2L)Exel8041*, (K) *ptcGAL4 WIZ-smo/swm*$^{Dh-1}$, (L) *ptcGAL4 WIZ-smo/ swm*^{F11}, (M) *ptcGAL4/10084R1* (*swm RNAi*), and (N) *ptcGAL4 WIZ-smo/ 10084R1*. Enhancement and suppression of the *smo RNAi* phenotype was scored as the distance between veins 3 and 4 in the proximal part of the wing near the anterior crossvein (see arrow in B). Ectopic vein tissue between veins 3 and 4 was seen in many genetic interactions with *smo RNAi* (*e.g.*, D, G, and J), but it did not correlate with enhancement or suppression.

reduced *smo* function due to expression of *smo RNAi* in the Hh-responsive intervein region of the wing. In developing this screen, we first established that knocking down components of the Hh signal transduction pathway by RNAi provides a reliable measure of Hh signaling. Injection of RNAi directed against components of the Hh signaling pathway strongly inhibits embryonic segmentation, and affected embryos recapitulate full loss-of-function phenotypes observed in null mutants (RAMIREZ-WEBER *et al.* 2000). To assess the efficacy of RNAi knockdown in the adult wing, we designed strains that target *smo* with RNAi.

smo RNAi expressed under the control of *ptc* produced partial proximal fusions of longitudinal veins 3 and 4 near the anterior cross vein (Figure 1, A and B; OGDEN *et al.* 2006). These fusions are similar to the defects that are observed with weak loss-of-function alleles of *fused* (*fu*), a gene that encodes a putative protein kinase that is required downstream of *smo* for Hh pathway activation. Although viable loss-of-function *smo* alleles have not been described, the fused vein phenotype is consistent with reduced *hh* signaling. This phenotype was obtained with either *T80GAL4* (ubiquitous expression in the wing disc; not shown) or *ptcGAL4*, but not when expression was restricted to the posterior compartment (with either *hhGAL4* or *enGAL4*). Wings with these latter genotypes were indistinguishable from wild type (not shown), indicating that the vein-fusion phenotype was dependent on expression of the RNAi in the anterior compartment cells that require Hh signaling.

Since the *ptcGAL4 smo RNAi* phenotype was both consistent and highly penetrant, its sensitivity to levels of Hh pathway components could be tested. The *smo RNAi* phenotype was completely suppressed by coexpression of a *smo* cDNA (Figure 1C), indicating that the wing phenotype was most likely due to RNAi-mediated reduction in *smo* expression. In contrast, reducing the number of functional *smo* genes by introducing an amorphic allele (either the deletion, *smo*^{D}, or the truncation generated by a stop codon in the second intracellular loop, *smo*^{3}) increased the extent of the 3–4 vein fusion. This is indicative of an enhanced effect (Figure 1D and data not shown; CHEN *et al.* 1998; ALCEDO *et al.* 2000). Reducing *hh* function (with either the *hh*^{AC} deletion or *hh*^{10} amorphic allele) enhanced vein fusion in *smo RNAi*-expressing flies, although to a lesser extent than the enhancement observed with *smo*^{3} or *smo*^{D} (Figure 1E and data not shown). We also reduced *hh* expression by introducing the mutant *en*^{E} (GUSTAVSON *et al.* 1996), which is deleted for the positive regulators of *hh* expression, *en* and *invected* (*inv*). Hemizygosity for *en/inv* enhanced the *smo RNAi* phenotype; although the

TABLE 1

Deficiencies on chromosomes 2 and 3 that enhance *smo RNAi*

Deficiency	Start	End	Interaction	Candidate gene
Df(2L)BSC37	22D2–3	22F1–2	Lethal	
Df(2L)GpdhA	25D7–E1	26A8–9	Enhancer	
Df(2L)cl7	25E1–2	26A7	Enhancer	
Df(2L)ED334	25F2	26B2	Weak enhancer	
Df(2L)E110	25F3–26A1	26D3–11	Enhancer	
In(2LR)DTD116[L]DTD24[R]	26A4–6	26C1–2	Weak enhancer	
Df(2L)BSC5	26B1–2	26D1–2	Weak enhancer	
Df(2L)ED353	26B2	26B5	Enhancer	
Df(2L)XE-3801	27E2	28D1	Enhancer	*mts*
Df(2L)RF	27E3–F	28B3–4	Weak enhancer	
Df(2L)BSC41	28A4–B1	28D3–9	Enhancer	*mts*
Df(2L)N22-14	29C1–2	30C8–9	Weak enhancer	
Df(2L)N22-5	29D1–2	30C4–D1	Weak enhancer	
Df(2L)30A-C	29F7–30A1	30C2–5	Weak enhancer	
Df(2L)N22-3	30A1–2	30D1–2	Enhancer	
Df(2L)gamma7	30A9–B1	30D2–F4	Weak enhancer	
Df(2L)BSC17	30C3–5	30F1	Weak enhancer	
Df(2L)J2	31B	32A	Enhancer	
Df(2L)J3	31D	31F	Enhancer	
Df(2L)J106	31D	31F2	Weak enhancer	
In(2LR)PL	31F	51C	Weak enhancer	
Df(2L)BSC32	32A1–2	32C5–D1	Weak enhancer	
Df(2L)BSC30	34A3	34B7–9	Enhancer	
Df(2R)E3363	47A	47F	Enhanced, small wing	
Df(2R)en-B	47E3	48A4	Enhancer	*en*
Df(2R)en-SFX31	48A	48B	Enhancer	*en*
Df(2R)RM2-1	54F2	56A1	Enhancer	
Df(2R)PC4	55A	55F	Weak enhancer	
Df(3L)M21	62F	63D	Enhancer	
Df(3L)HR119	63C2	63F7	Enhancer	
Df(3L)vin6	68C8–11	69A4–5	Enhancer	
Df(3L)Exel6116	68F2	69A2	Enhancer	
Df(3L)vin5	69A2–3	69A1–3	Enhancer	
Df(3R)M-Kx1	86C1	87B1–5	Weak enhancer	
Df(3R)Exel6162	87A1	87B5	Lethal	
Df(3R)ry615	87B11–13	87E8–11	Weak enhancer	
Df(3R)Exel8157	87D8	87D10	Weak enhancer	
Df(3R)Exel6193	94D3	94E4	Enhancer	*hh*
Df(3R)BSC56	94E1–2	94F1–2	Enhancer	*hh*
Df(3R)96B	96A21	96B8–10	Enhancer	
Df(3R)Espl3	96F1	97B1	Enhancer	

Note that there are no multigenic deficiencies that span the *smo* locus.

enhancement was less than with either the *smo* or *hh* mutants, it was reproducible (Figure 1F). Suppression of the *smo RNAi* phenotype was observed when *ptc* function was reduced in ptc^{10} heterozygotes (Figure 1G). ptc^{10} is an EMS-induced null allele (Ramirez-Weber *et al.* 2000). Since Ptc is a negative regulator of Hh signaling, we conclude that *smo RNAi* assay is a reliable indicator for the pathway.

Identification of deficiencies that modify *smo RNAi*: We challenged the *smo RNAi* phenotype with 216 lines from the Bloomington Drosophila Stock Center deficiency collection for chromosomes 2 and 3. In aggregate, these lines are estimated to delete >90% of the autosomal euchromatin. Since their diverse genetic backgrounds are likely to affect the *smo RNAi* phenotype, each line was crossed into a common background prior to testing. Wing phenotype was monitored among F_2 progeny, and since flies carrying the deficiency could be distinguished from nondeficiency bearing flies, each cross was internally controlled for subtle background effects. Crosses were scored by comparing the vein morphology of a minimum of 25 flies of each genotype. Every deficiency observed to enhance or suppress the *smo RNAi* phenotype was retested, and regions that gave consistent

TABLE 2

Deficiencies on chromosomes 2 and 3 that suppress *smo RNAi*

Deficiency	Start	End	Interaction	Candidate gene
Df(2L)cact-255rv64	35F–36A	36D	Suppressor	
Df(2L)TW50	36E4–F1	38A6–A7	Suppressor	*swm*
Df(2L)pr-A16	37B2–12	38D2–D5	Suppressor	*swm*
Df(2L)TW158	37B2–B8	37E2–F1	Suppressor	*swm*
Df(2L)VA17	37C1	37F5	Suppressor	*swm*
Df(2L)VA12	37C2–5	38B2–C1	Suppressor	*swm*
Df(2L)Sd77	37D1–D2	38C1–C2	Suppressor	*swm*
Df(2L)Sd37	37D2–D5	38A6–B2	Suppressor	*swm*
Df(2L)pr-A14	37D2–D7	39A4–A7	Suppressor	*swm*
Df(2L)E55	37D2–E1	37F5–38A1	Suppressor	*swm*
Df(2L)Exel8041	37D7	37F2	Suppressor	*swm*
Df(2R)H3C1	43F	44D3–D8	Suppressor	
Df(2R)44CE	44C4	44E4	Suppressor	*ptc*
Df(2R)H3E1	44D1–D4	44F12	Suppressor	*ptc*
Df(2R)H3D3	44D1–4	44F4–5	Suppressor	*ptc*
Df(2R)Exel8047	44D4	44D5	Suppressor	*ptc*
Df(2R)Exel7098	44D5	44E3	Suppressor	*ptc*
Df(2R)CX1	49C1–4	50C23–D1	Weak suppressor	
Df(2R)X58-8	58B3	59A1	Suppressor	
Df(2R)59AD	59A1–A3	59D1–D4	Suppressor	
Df(3L)CH39	64	65B5–C1	Weak suppressor	
Df(3L)ED210	64B9	64C13	Weak suppressor	
Df(3L)CH18	64B–C	65B5–C1	Weak suppressor	
Df(3L)ZN47	64C	65C	Suppressor	
Df(3L)CH20	64D1–2	65C3	Suppressor	
Df(3L)Exel6107	64E5	64F5	Suppressor	
Df(3L)vin2	67F2–F3	68D6	Weak suppressor	
Df(3L)ED4470	68A6	68E1	Weak suppressor	
Df(3L)D-5rv12	70C2	72A1	Suppressor	
Df(3R)D605	97E3	98A5	Suppressor	
Df(3R)R38.3	97E3–11	98A	Suppressor	

effects were characterized further. If available, additional genomic deletions in the region were tested, and any available lines harboring mutations in genes uncovered by the smallest deletion were tested for enhancement or suppression. This analysis entailed >2500 crosses.

The deficiencies that modify the *smo RNAi* phenotype are listed in Tables 1 and 2. Figure 2 depicts the cytological positions of deficiencies and mutations that either enhance (red) or suppress (blue) the 3–4 veinfusion phenotype. Among the deficiencies identified in the screen are ones that removed the known Hh pathway components *en*, *ptc*, and *hh*. (There are currently no multigenic deficiencies available for the *smo* region.) The *en*, *ptc*, and *hh* deficiencies produced phenotypes that mimicked the mutant alleles of these genes. In addition to these regions, there were nine that sup-

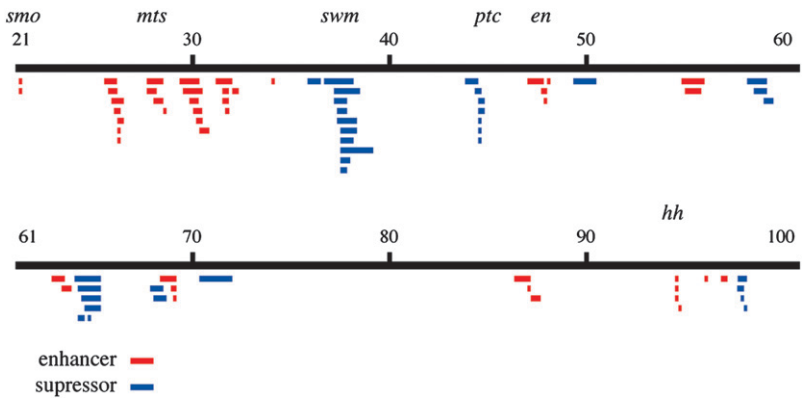

FIGURE 2.—Results of the *smo RNAi* enhancer-suppressor screen. Chromosomes 2 and 3 are depicted graphically as black lines. Below, deletions and mutant chromosomes that enhance (red) or suppress (blue) this phenotype are indicated with bars. Cytological locations are marked, and candidate enhancer and suppressor genes are indicated.

pressed and thirteen that enhanced the vein-fusion phenotype. We have identified protein-encoding genes that affect Hh signaling in two of these regions.

***microtubule star*:** The screen mapped a mild enhancement function to the 28A–D interval using deficiencies *Df(2L)XE-3801* and *Df(2L)BSC41* (Table 1, Figure 1H, and data not shown). This region contains *microtubule star* (*mts*; CG7109), and we confirmed that these deficiencies fail to complement *mts* (Wassarman *et al.* 1996). We tested five *mts* alleles in the *smo RNAi* assay. One, $mts^{XE\text{-}2258}$, recapitulated the effects of the deficiencies by weakly enhancing the phenotype (Figure 1I); it has a 16-bp deletion that includes the translation start (Wassarman *et al.* 1996). None of the four *P*-element insertions ($P\{lacW\}mts^{k12502}$, $P\{PZ\}mts^{02496}$, $P\{PZ\}mts^{05559}$, and $P\{lacW\}mts^{s5286}$) yielded significant enhancement.

To test $mts^{XE\text{-}2258}$ for effects on Hh signaling with an assay that is independent of *smo RNAi* and the *GAL4* system, crosses were made to the *hh* allele, hh^{Mrt}. hh^{Mrt} is a dominant gain-of-function allele that causes ectopic expression of *hh* along the dorsal/ventral border in the anterior compartment of wing discs; it causes overgrowth of anterior distal wing structures (Felsenfeld and Kennison 1995). Reducing the dosage of *mts* by introducing $mts^{XE\text{-}2258}$ or either of the two *mts* deficiencies strongly suppressed the hh^{Mrt} wing overgrowth, resulting in wings that approached wild type. In control crosses, over two-thirds of the $hh^{Mrt}/+$ wings showed overgrowths (class I, 0%; II, 13%; III, 71%; and IV, 16%). When mts function was reduced in $mts^{XE\text{-}2258}/+$; $hh^{Mrt}/+$, the percentage of wings with overgrowths was reduced by >50% (class I, 32%; II, 36%; III, 28%; and IV, 4%). At the same time, the percentage of wings with normal overall shape (classes I and II) increased from 13 to 68%. *mts* encodes the catalytic subunit of protein phosphatase type 2A (PP2A); its name derives from the unusual appearance of centrosomal microtubules in mutant embryos (Snaith *et al.* 1996). Consistent with our *in vivo* data, *in vitro* experiments from an RNAi-based screen of Drosophila CL8 cultured cells also suggest that *mts* is required for maximal Hh pathway activation (Nybakken *et al.* 2005).

***second mitotic wave missing*:** The screen identified a strong suppression function in the 37D7–F1 interval. Nine overlapping deletions were identified in this region that suppressed the *smo RNAi* phenotype (Table 2); these define a region that is predicted to include 32 genes. Among 13 RNAi lines and 12 point mutants in this region that we tested, four suppressed *smo RNAi* in the manner of the smallest deletion, *Df(2L)Exel8041* (37D7–37F2; Figure 1J and data not shown). These four are 10084R1 and 10084R2 (further examination revealed that these two *GAL4*-driven RNAi lines are isogenic), $swm^{37Dh\text{-}1}$ and $swm^{37Dh\text{-}9}$ (Figure 1, K, M, and N, and data not shown). $swm^{37Dh\text{-}1}$ and 10084R2 suppressed expression of dominant negative smo^{5A}, but not *cut RNAi* expression (data not shown).

The *swm* gene (CG10084; 37E4) was first identified genetically as a recessive lethal complementation group in a screen for new alleles of *ref(2)P* (Gay and Contamine 1993). *ref(2)P* determines susceptibility to Sigma virus. Nine ethyl methanesulfonate-induced *swm* alleles, including $swm^{37Dh\text{-}1}$ and $swm^{37Dh\text{-}9}$, were isolated. More recently, *swm* alleles [$S(rux)2B^1$ and $S(rux)2B^2$, aka swm^1 and swm^2] were identified in a screen for suppressors of the CDK inhibitor gene *roughex* (*rux*; Dong *et al.* 1997; Foley and Sprenger 2001). *S(rux)2B* is a recessive lethal that partially rescues a *rux* roughened eye phenotype (B. Thomas, personal communication; Dong *et al.* 1997). We confirmed that $swm^{Dh\text{-}1}$ increases the size of the eye and partially suppresses the rux^1 rough eye phenotype (data not shown).

swm is predicted to produce two transcripts that have identical open reading frames and are distinguished by alternative transcriptional start sites. These transcripts putatively encode a 1062 amino acid protein. Their coding regions distribute over 5 exons that are preceded by an alternatively-spliced 5′ noncoding exon; their five introns are small, totaling <600 nucleotides. The Swm protein is predicted to have four sequence motifs. A CCCH-type Zn^+ finger domain (residues 364–398) might function in nucleic acid binding or in protein–protein interactions (Figure 3A, yellow). Residues 574–632 might represent an RNA-binding RNA recognition motif (RRM; Figure 3A, blue), although it might function in nucleotide binding or as a structural domain. Two nuclear localization sequences are predicted (residues 242–250 and 748–769). Expression of a N-terminally tagged GFP–Swm fusion protein in transfected S2 cells generated strong nuclear fluorescence (Figure 6, A–C), consistent with nuclear localization of Swm. Expression in salivary glands was also predominantly nuclear (Figure 6D).

BLAST searches (Altschul *et al.* 1990) identified several potential Swm homologs in animal genomes, as well as more distantly related proteins in plants and fungi. The mouse and human genomes each have two putative homologs. The two human gene products are RBM26 (also known as cutaneous T-cell lymphoma tumor antigen se70-2) and RBM27 (also known as peri-implantation stem cell protein 1 for mouse, and KIAA1311 and POU domain, class IV, transcription factor 3 for human; Kavanagh *et al.* 2005); both have the same predicted domain structure as Drosophila Swm. Their strongest sequence similarities are in the amino terminus, zinc finger, RRM domain, and acidic carboxy terminus (Figure 3B). The mouse and human RBM26 proteins are almost identical to each other, as are the corresponding RBM27 proteins. Multiple splice variants of these vertebrate genes have been identified.

We monitored expression of Drosophila *swm* by *in situ* hybridization and detected transcripts at all stages that were examined (Figure 4). Expression was strong in cellularized embryos and was enhanced along the

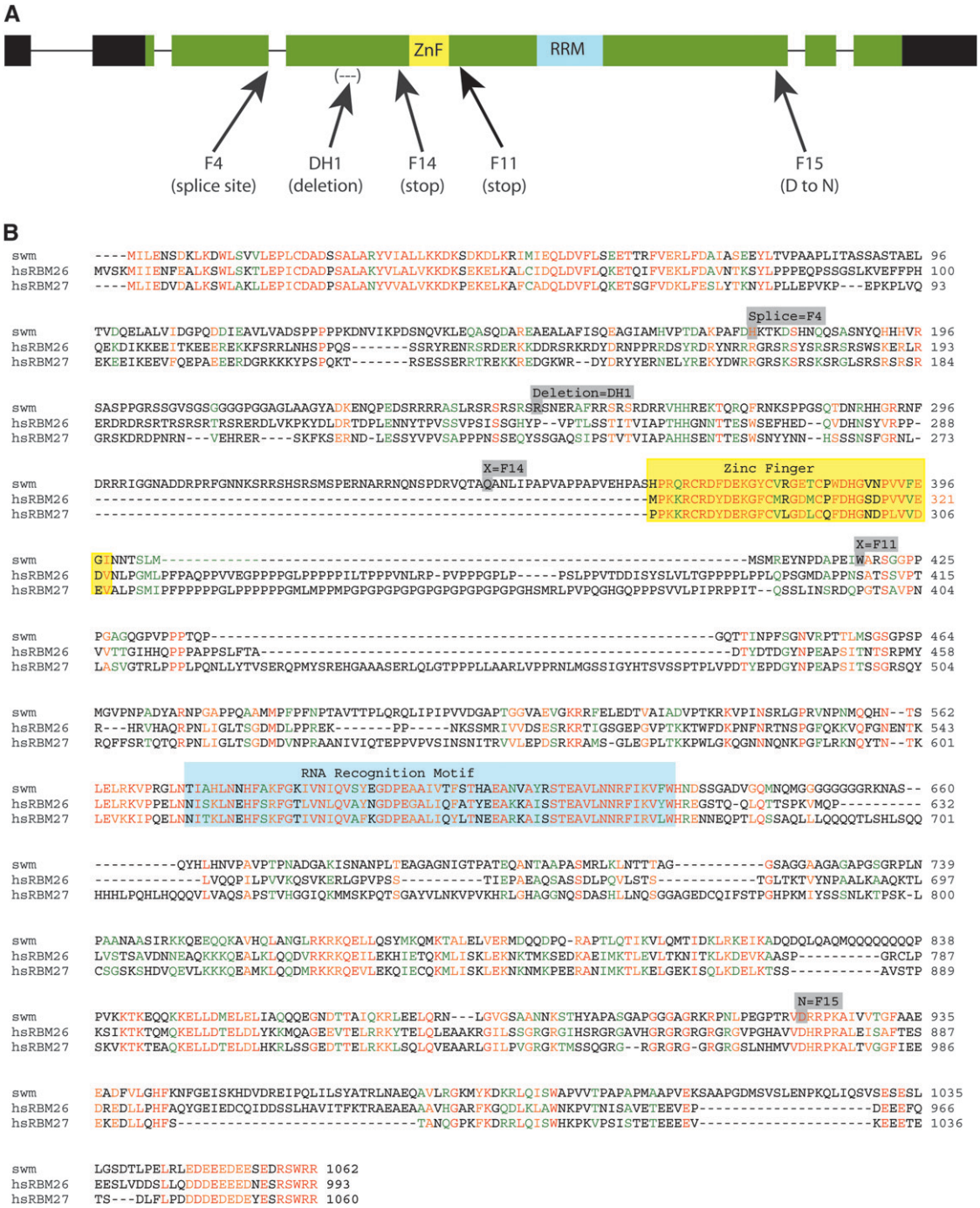

FIGURE 3.—The *swm* locus and sequence. (A) The *swm* locus has six exons in its *swm-RA* transcript (thick bars) and five introns (thin lines). The *swm-RB* transcript is predicted (FlyBase) to have only five exons and an alternative transcriptional start site within intron one (not shown). Both transcripts have the same predicted protein coding region (1062 amino acids, green). Noncoding regions of exons one, two, and six are in black. Two putative functional domains are shown: a CCCH-type Zn^{+} finger (yellow) and an RNA recognition motif (blue). Mutations in five *swm* alleles are indicated. (B) Swm protein aligned with human RBM-26 (GenBank, EAW80593) and RBM-27 (GenBank, Q9P2N5). Identity (red), strong similarity (orange), weak similarity (green), no similarity (black), Zn^{+} finger domain (yellow box), RRM (blue box). Mutations in *swm* alleles, in boldface type: swm^{F4} (after D175 GT to AT, the last residues before the splice site); $swm^{Dh\text{-}1}$, 157-bp deletion at S249; swm^{F14}, Q314 to stop (CAA to TAA); swm^{F11}, W418 to stop (TAG to TGG); swm^{F15}, D923N.

ventral midline. Segmental stripes were evident at germband retraction. Late in embryogenesis, *swm* expression appeared to be ubiquitous. In third instar larval tissues, strong *swm* expression was observed in imaginal discs, salivary gland, optic lobe, fat body, and in the wreath cells and gastric caecae of the gut.

Isolation and analysis of *swm* alleles: To isolate additional *swm* mutants, we carried out an F_2 screen for

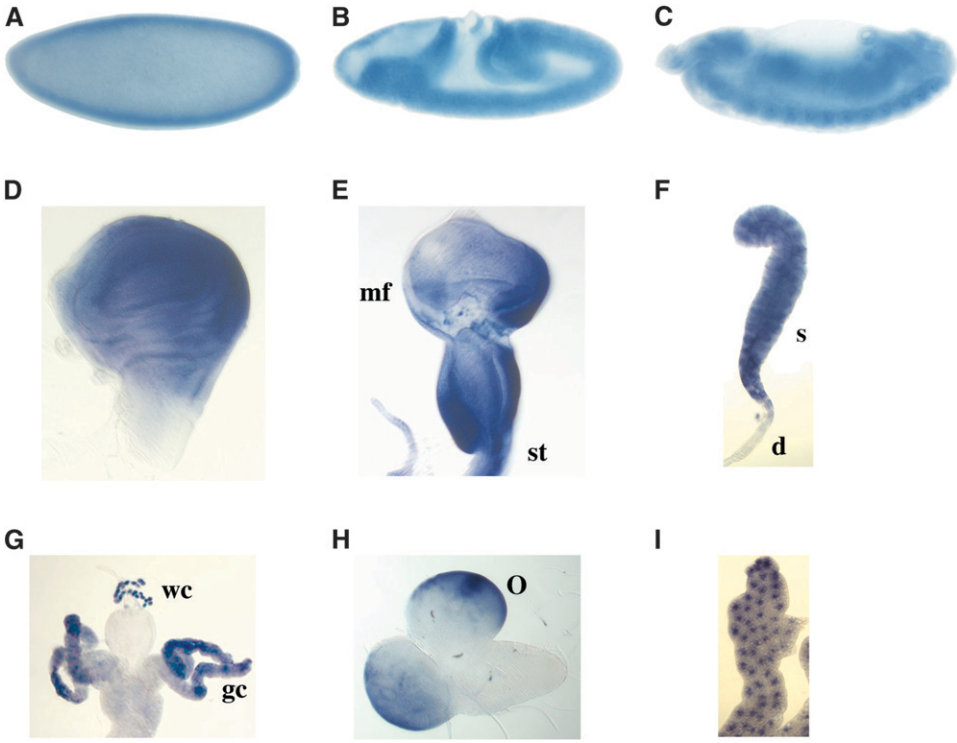

FIGURE 4.—*swm* expression in embryos and larva. *In situ* hybridization reveals *swm* expression in (A) precellular embryo, (B) germ-band extension embryo, (C) germ-band retraction embryo, (D) third instar wing disc (posterior is on the right), (E) eye/antennal disc (mf, morphogenetic furrow; st, stalk), (F) salivary gland (s, secretory cells; d, duct cells), (G) gut (gc, gastric caecae; wc, wreath cells), (H) larval brain (o, optic lobe), and (I) larval fatbody.

noncomplementing alleles of $swm^{37Dh\text{-}1}$. We used an isogenized, viable second chromosome carrying *FRT40A* that was also marked at 30A with a viable w^+ insertion. We found five noncomplementing chromosomes among ~4000 progeny that were screened.

To determine if the noncomplementing chromosomes have mutant *swm* alleles, *swm* coding sequences were determined from the new lines as well as from both the isogenized starting strain, $swm^{37Dh\text{-}1}$ and from a *swm* cDNA obtained from the Berkeley Drosophila Genome Project collection. The wild-type isogenized chromosome differed from both the *swm* cDNA and GenBank *swm* sequences at two positions. Both are likely to be polymophisms; one is silent in codon 996 (ACA to ACT) and the other (TCC to GCC) changes serine 402 to alanine. The $swm^{37Dh\text{-}1}$ allele has a 157-bp deletion in exon 4 that shifts the reading frame at Serine 249 (Figure 3, A and B, mutations are in gray). Mutations were found within the *swm* transcription unit of four mutagenized chromosomes. The swm^{F11} and swm^{F14} alleles have stop codons at residues 418 and 344, respectively, and are predicted to produce truncated proteins. The swm^{F4} allele has a G-to-A mutation in the first base of the 5′ splice site of intron 3. These three new *swm* alleles, all of which are predicted to produce proteins deleted of the RRM domain, are strong suppressors of *smo RNAi* (Figure 1, J–L and data not shown). They are presumed to be nulls.

Heteroallelic combinations of the null *swm* alleles (swm^{F4}, swm^{F11}, swm^{F14}, $swm^{37Dh\text{-}1}$, $swm^{37Dh\text{-}9}$, and *Df(2L)Exel8086*) died in L3. Mutant larvae were severely developmentally delayed, and most had wing discs that were <25% the size of wild type.

A missense mutation was identified in swm^{F15} (D923N; Figure 3B). D923 is conserved in both human Rbm26 (D873) and Rbm27 (D972); it may be in a casein kinase I phosphorylation site. Although swm^{F15} is recessive lethal, rare transheterozygous escapers with $swm^{37Dh\text{-}1}$, swm^{F14}, and *Df(2L)Exel8041* were recovered. In addition, swm^{F15} is not a dominant suppressor of *smo RNAi*. We therefore conclude that swm^{15} retains some function and is hypomorphic.

swm^{F15} adult escapers (*e.g.*, $swm^{F15}/swm^{Dh\text{-}1}$, swm^{F15}/swm^{F14}, and $swm^{F15}/Df(2L)Exel8041$) were normal size, but were abnormal in several respects. Ocelli were reduced or absent; cephalic macrochaetae were frequently missing; the base of the aristae were frequently enlarged, resembling a weak aristapedia phenotype; eyes were rough; and wings, though normal in size, had ectopic vein tissue and an increased distance between veins 3 and 4 (Figure 6, G and I and data not shown). In swm^{DH1}/swm^{F15} wings, the region between veins 3 and 4 was 12% larger than the same region in wild-type wings. The 3–4 intervein region comprised 23 ± 1%, ($n = 23$) of a swm^- wing *vs.* 21 ± 0.3% of a wild-type wing ($n = 11$). These two populations are different by Student's *t*-test, $P < 3.6 \times 10^{-10}$. Wings also had a weak wing hair polarity phenotype that is described below.

To investigate how cells that lack *swm* function develop in the wing disc, three methods were used to induce clones of *swm* mutant alleles. First, negatively marked clones of two *swm* amorphic alleles (swm^{F4} and swm^{F14}) were induced such that the clones lacked GFP expression and twin spots had increased fluorescence relative to nonrecombined cells. Despite an abundance of large twin spots, no *swm* clones were found. Second,

the MARCM technique (Lee *et al.* 2000) was used to positively mark clones of four alleles (swm^{F4}, swm^{F11}, swm^{F14}, and swm^{F15}). swm^{F4}, swm^{F11}, and swm^{F14} clones were identified, but they were small (1–2 cells) and few in number. swm^{F15} clones were slightly larger (up to 8 cells) and were slightly more frequent. Third, M^+ mutant clones of three alleles (swm^{F4}, swm^{F11}, and swm^{F14}) were induced *in trans* with $M(2)24F^1$ to endow *swm* mutant cells with a growth advantage. Neither the number nor size of clones increased. We conclude that loss of *swm* function is cell lethal in *swm*/+ discs. Although mutant cells cannot survive in a background of *swm*/+ cells, the survival of swm^{F15} transheterozygotes indicates that *swm* insufficiency is not generally cell lethal. We do not understand the basis for this behavior. We investigated whether *swm* function is required in the germline. Although germline clones of the hypomorph swm^{F15} generated fertile eggs and swm^{F15}/+ adults from such eggs were phenotypically normal, no swm^{F11} or swm^{F14} mutant eggs were recovered. In crosses to $swm^{Dh\text{-}1}$/*CyO-WeeP*, $swm^{F15}/swm^{Dh\text{-}1}$ progeny of swm^{F15} female germline clones were larval lethal like other *swm* transheterozygotes.

***swm* is a negative regulator of Hh signaling:** Genetic and molecular analyses provided evidence indicating that *swm* negatively regulates Hh signaling. In the sensitized *smo RNAi* background, hemizygosity for *swm* strongly and consistently suppressed the wing vein phenotypes characteristic of reduced Hh signaling (Figure 1, J–L). *swm RNAi* generated more extreme phenotypes both alone and in combination with *smo RNAi* (Figure 1, M and N), with a reduction of the distance between veins 2 and 3 reminiscent of ectopic expression of Hh or a dominant negative form of Ptc (Tabata and Kornberg 1994; Porter *et al.* 1996; Ramirez-Weber *et al.* 2000; Lu *et al.* 2006;). When driven by *ptcGAL4* at 29°, the *swm RNAi* phenotype was completely penetrant, and when coexpressed with *smo RNAi* the fused wing phenotype was suppressed in every fly. In control crosses, *swm RNAi* did not suppress the wing margin phenotype caused by *cut RNAi* expression (data not shown), showing that the effects of *swm RNAi* are not targeted generally and nonspecifically to the RNAi pathway.

Expression of a dominant negative Smo protein, Smo^{5A} (Collins and Cohen 2005), causes wing vein fusions that are similar to *smo RNAi*. This mutant protein has alanines substituted for serines and threonines in the C-terminal cytoplasmic tail that are phosphorylated upon Hh activation, and its expression in the wing partially blocks Hh signaling (Collins and Cohen 2005). Reducing *swm* function (*e.g.*, $swm^{37Dh\text{-}1}$/+ or *swm RNAi*) partially suppressed the vein-fusion phenotype of smo^{5A}-expressing flies (not shown); the capacity for $swm^{37Dh\text{-}1}$ hemizygosity to counteract the effects of reduced Hh signaling is not specific to *smo RNAi*.

We also examined the *swm* insufficiency phenotype in a Hh gain-of-function background. As noted above, in the hh^{Mrt} mutant, Hh is ectopically expressed along the dorsal ventral border of the wing disc and the majority of wings develop with anterior overgrowths (class I, 0%; II, 13%; III, 71%; and IV, 16%; see Figure 5, A and B). $swm^{37Dh\text{-}1}$/+; hh^{Mrt}/+ wings had more severe overgrowths (class I, 0%; II, 5%; III, 30%; and IV, 65%; see Figure 5, C and D). While severely distorted class IV wings were rare in hh^{Mrt}/+ flies, the majority of $swm^{37Dh\text{-}1}$/+; hh^{Mrt}/+ wings were in this class. Antibody staining of the Hh targets Ptc and Ci revealed patterns that were consistent with elevated Hh signaling. Levels of Ptc and Ci are normally elevated at the A/P compartment border, and both were also present along the D/V border in the anterior compartment where Hh is ectopically expressed in hh^{Mrt} discs (Figure 5, E, F, H, and I). In $swm^{37Dh\text{-}1}$/+; hh^{Mrt}/+ discs, expression of both proteins was greatly enhanced along the D/V border (Figure 5, G and J).

Cell polarity and cell-size defects in *swm* mutants: In addition to the abnormalities in the wings noted above, wings of the three heteroallelic *swm* genotypes that produced escapers had subtle wing hair polarity defects. Whereas the orientation of hairs in wild-type wings is highly regular, with hairs of neighboring cells having almost identical proximodistal orientations, most wings of *swm* mutants ($swm^{F15}/swm^{Dh\text{-}1}$, 70%; swm^{F15}/swm^{F14}, 76%; $swm^{F15}/Df(2L)Exel8041$, 100%) had patches that deviated 30–40% from the normal orientation. A mild form of this phenotype was also evident in posterior wing compartments in which swm function was reduced with *enGAL4 swm RNAi* (data not shown). These patches did not generate "whorls" characteristic of mutants in planar cell polarity (PCP) genes, but had hairs with orientations that were noticeably askew (Figure 6, G and H) and had occasional cells with multiple wing hairs (not shown). We also observed patches of misoriented hairs in wings that had not been mounted under a coverslip, establishing that the phenotype is not an artifact of preparation. We did not find an effect on bristle orientation or on the orientation of hairs in the abdomen.

swm and wild-type wings were approximately equal size, but the density of wing hairs in *swm* wings was less than wild type. As each cell normally produces a single distal wing hair, the number of hairs in a given area provides a measure of the number and the size of cells. In equivalent areas between veins 4 and 5 that we chose for purposes of comparison, *swm* wings had ~20–28% fewer cells (swm^{F14}/swm^{F15}, 76 ± 5 cells; $swm^{F15}/swm^{Dh\text{-}1}$, 68 ± 8 cells; wild type, 95 ± 3 cells; $n = 11$ wings), indicating that reduction of *swm* causes an increase in wing cell size.

DISCUSSION

The screen for effectors of the Hh pathway: This screen identified twenty-six autosomal regions that

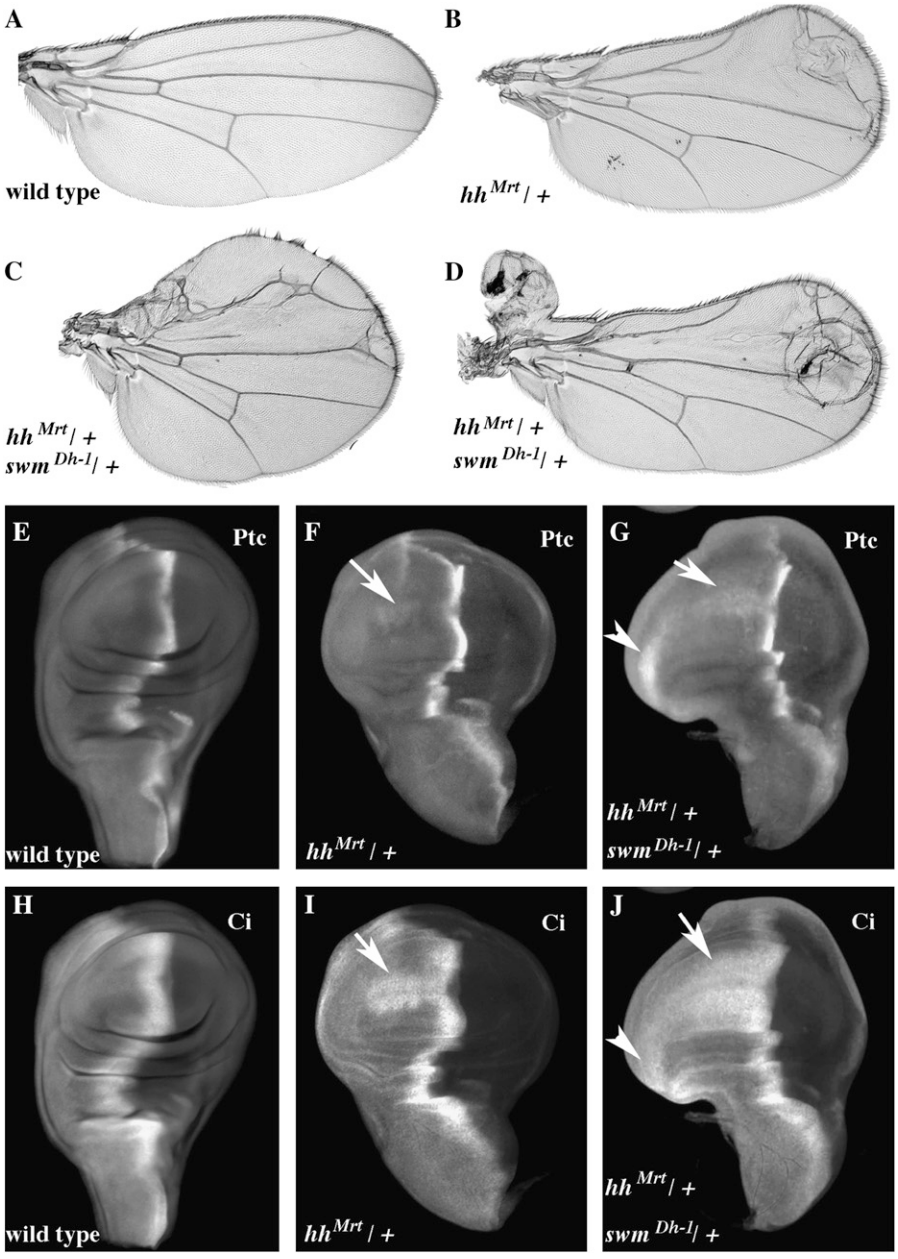

FIGURE 5.—hh^{Mrt} is enhanced by *swm*. Wings: (A) wild type, (B) $hh^{Mrt}/+$, (C) and (D) $swm^{Dh\text{-}1}/+$; $hh^{Mrt}/+$. Third instar wing imaginal discs were stained for Ptc (E, F, and G) or Ci (H, I, and J) protein. Genotypes are as follows: (E and H) wild type; (F and I) $hh^{Mrt}/+$; and $swm^{Dh\text{-}1}/+$; (G and J) $hh^{Mrt}/+$. The arrows indicate ectopic expression of Ptc and Ci in the anterior compartment along the dorsal ventral compartment boundary.

modified a smo hypomorphic phenotype in a dosage-sensitive manner. Two aspects of its design were key to its success. First, its two-generation crossing scheme eliminated background effects by homogenizing the genetic backgrounds of both experimental and control flies. It also generated reasonably large numbers of both classes of progeny so that a good estimate of an average phenotype could be obtained. These features allowed us to monitor subtle variations in wing vein morphology, despite the significant strain differences among the many lines we tested. Second, its high scoring threshold rendered it relatively insensitive to changes in Hh signaling strength, thereby helping to submerge weak influences. Key to this property was the *ptcGAL4* driver that was used to express *smo RNAi*; it functioned in part as a "genetic buffer." Since *ptcGAL4* is itself responsive to Hh, a modifier that increased Hh signaling would also be predicted to increase the expression of *ptcGAL4* and *smo RNAi*, while a modifier that decreased Hh signaling might be expected to decrease the expression of the *ptcGAL4* and *smo RNAi*. *ptcGAL4* therefore buffered against changes in signaling strength and decreased the effects of genetic factors that enhance or suppress signaling; as a consequence, only highly penetrant and consistent phenotypes were scored.

Our screen netted many of the known core components of the Hh signaling pathway, including *smo*, *ptc*, *hh*, and *en*. We report on *mts* and *swm*, two genes whose haplo-insufficiency phenotypes were sufficiently strong to score above the threshold set by our genetic tests.

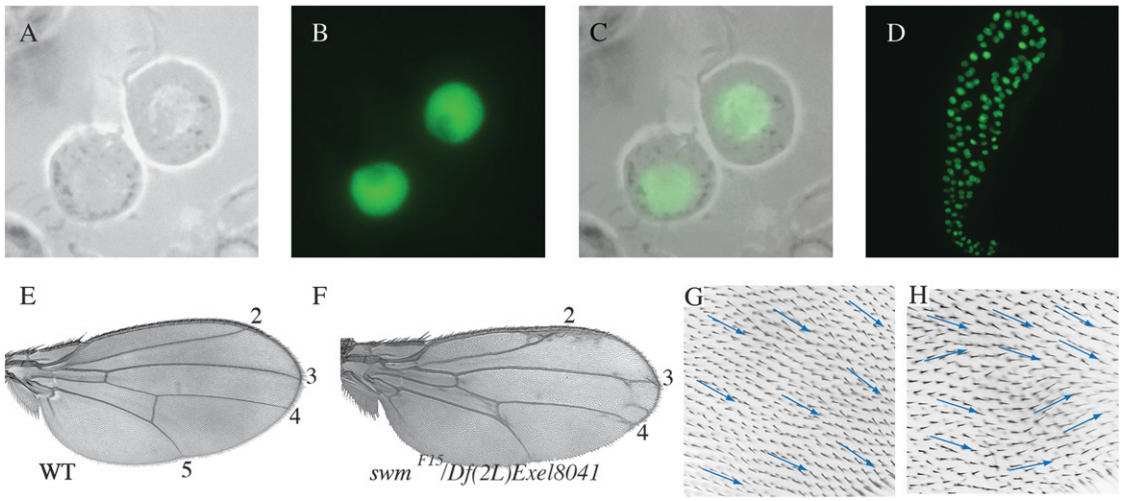

Figure 6.—Swm localization and function. (A–C) S2 cells expressing GFP–Swm localize GFP fluorescence to nuclei (A, phase contrast; B, fluorescence; C, merge). (D) GFP–Swm localized to nuclei in third instar salivary glands. (E and F) Wing from a *swm*^{F15}*/Df(2L)Exel8041* escaper (F) has intervein regions 3–4 expanded and misoriented hairs (H), in contrast to wild-type control (E and G).

Many other known regulators of Hh signaling were not identified in our screen. There are perhaps multiple reasons, including the high scoring threshold of the *smo RNAi* screen, or the possibility that not all pathway regulators have haplo-insufficiency phenotypes. *skinny hedgehog* or *suppressor of fused* were not included among those identified in the screen, despite the fact that deficiencies that removed them interacted with *smo RNAi*. The reason is that mutant alleles of these genes that were tested did not yield similar interaction phenotypes. Since we observed many examples of interaction between null alleles of Hh pathway regulators and *smo RNAi* but consistent failure of hypomorphic alleles to interact, we do not view that lack of interaction as evidence against a gene being a *smo RNAi* enhancer/suppressor. The possibility that stronger alleles might interact cannot be discounted. We were surprised that hemizygosity of *cos2* did not show an interaction with *smo RNAi*. This could be because it is not haplo-insufficient in our particular assay or because of the complex positive and negative roles *cos2* plays in Hh signaling. Finally, there was no apparent overlap between the regions we identified and the mutant lines that were identified in previous screens for modifiers of Hh phenotypes (Haines and van den Heuvel 2000; Collins and Cohen 2005); the *smo RNAi* assay may be less sensitive but more specific.

***microtubule star*:** *mts* lies within 1 of 16 regions that enhanced the *smo RNAi* phenotype, suggesting that its wild-type function augments the Hh response. *mts* encodes the catalytic (C) subunit of PP2A, a heterotrimeric phosphatase that has two regulatory subunits, B and B′. It was previously identified as a Hh pathway regulator in CL8 cells (Nybakken *et al.* 2005); our work now provides *in vivo* evidence for a role in Hh signaling during development. Three proteins in Hh signal transduction have been shown to be functionally phosphorylated. Phosphorylation of the Smo C terminus is induced by Hh and is required for surface accumulation of Smo and normal activation of the pathway (Zhang *et al.* 2001, 2004; Apionishev *et al.* 2005). Thus, reduction of PP2A activity and increased phosphorylation of Smo would not be expected to decrease Hh signaling and enhance the *smo RNAi* phenotype. Other possible targets of Mts are Ci and Cos2. Phosphorylation of Ci by PKA, casein kinase 1α, and GSK3β is required to convert Ci from its full-length form to its transcriptional repressor form, Ci-75 (Chen *et al.* 1998; Jia *et al.* 2002; Price and Kalderon 2002). Hh signaling blocks this proteolytic transformation and also promotes conversion of Ci to an activator form (Aza-Blanc *et al.* 1997). A decrease in phosphatase activity might increase levels of phosphorylated Ci to effect enhanced conversion to Ci-75 and reduced levels of Ci activator. Levels of Hh signaling would be predicted to decrease. Alternatively, Mts might control phosphorylation of Cos2 by Fu. Phosphorylation of Cos2 prevents its binding to Smo and release of Smo from Cos2 increases the cell surface accumulation of Smo that is necessary for pathway activation (Denef *et al.* 2000; Liu *et al.* 2007). Therefore, a reduction of Smo on the plasma membrane due to loss of PP2A activity might attenuate Hh pathway activation.

While the catalytic subunit of PP2A carries enzymatic phosphatase activity, the substrate specificity of PP2A is directed by its regulatory subunits. The phenotypes of mutants in genes that encode the B and B′ regulatory subunits of PP2A, *twins* and *widerborst* (*wdb*), respectively, are interesting to consider in the context of Hh signaling. Wing discs in the *twins*^{P} mutant have mirror symmetrical posterior compartment duplications that are associated with ectopic compartment borders (Uemura

et al. 1993). Symmetric wing duplications have also been observed after ectopic expression of Hh or Dpp (Zecca *et al.* 1995 and reviewed in Tabata and Takei 2004), or after loss of *en/inv* induces an ectopic compartment border (Tabata *et al.* 1995). Since loss of PP2A function should reduce Hh signaling, it is not obvious how loss of the B *twins* regulatory subunit leads to an ectopic signaling center. Understanding this interesting aspect of the twins phenotype warrants further investigation.

Misexpression of PP2A can cause cell planar polarity defects in the wing. Misexpression of *mts*, *wdb*, or mutant alleles of these genes disrupted wing hair polarity (Hannus *et al.* 2002). Like *mts*, reducing *wdb* expression with RNAi reduced Hh signaling in CL8 cells (Nybakken *et al.* 2005). This evidence, as well as the wing hair polarity phenotype of *swm* mutants, raises the possibility that PP2A links Hh signaling with cell polarity. The PCP and Hh pathways may be parallel and independent if PP2A activity is simply common to both, but evidence that Hh is required to establish PCP in the Drosophila embryonic and adult epidermis has recently been described (Colosimo and Tolwinski 2006; Lawrence *et al.* 2007). As discussed below, the phenotype of *swm* mutants provides additional evidence for an association of Hh signaling with cell polarity.

***second mitotic wave missing*:** *swm* was first identified as *l(2)37Dh* by Gay and Contamine (1993) in a screen for recessive lethal alleles within *Df(2L)E55* (37D2–38A1). It was shown to exhibit synthetic lethality as an enhancer of *Minutes*. Among the mutant chromosomes from our screen that failed to complement *swm*, one had a *Minute*-like phenotype. No changes in the *swm* coding sequence were found in this mutant; rare escapers that eclosed as heterozygotes with our verified *swm* alleles had a variety of phenotypes including loss of ocelli, thin macrochetae, and deformed legs. In contrast to *swm* mutant escapers, however, both their eyes and wings were phenotypically normal (not shown).

More recently, *swm* was identified as a suppressor of the *roughex* eye phenotype (Dong *et al.* 1997). Alleles of *ptc* were also isolated in this screen (B. Thomas, personal communication). We confirmed these interactions between *rux*, *ptc*, and *swm* (data not shown). Since Ptc is a negative regulator of the Hh pathway and *ptc* mutations are therefore likely to elevate Hh signaling, and since Hh plays a key role in eye morphogenesis, the rux phenotype is apparently sensitive to Hh levels. We therefore interpret the identification of both *ptc* and *swm* mutants as *rux* suppressors as a consequence of the same mechanism—an increase in Hh signaling caused by a decrease in the level of a negative regulator.

Our results provide several additional lines of evidence that *swm* negatively regulates Hh signaling. *swm* mutants dominantly suppress smo hypomorphic phenotypes (*smo RNAi* and smo^{5A}; Figure 1 and data not shown), enhance a Hh gain-of-function phenotype (hh^{Mrt}; Figure 5), and increase targets of Hh signaling such as Ptc and Ci (Figures 5 and 6). These effects on Hh signaling seem to occur through swm activity in the anterior compartment since *swm RNAi* expressed in these cells is sufficient to suppress *smo RNAi*. Although these interactions implicate Swm, we have not determined how and where Swm impacts signal transduction or what its molecular function might be. Swm protein has features suggestive of a function in nucleic acid metabolism—it has a putative RRM RNA binding domain and a CCCH Zn^{+} finger (Figure 3), and a GFP–Swm fusion we examined localized to nuclei in cultured cells (Figure 6). Presumably, Swm affects expression, production, or presentation of proteins involved in Hh signaling or signal transduction. However, *swm* function is not specific to Hh signaling, since many aspects of the phenotype (*e.g.*, ectopic venation, wing hair polarity, cell size, and interaction with *Minutes*) are not attributable to defects in Hh signaling.

swm is expressed broadly in both embryos and larvae, and in wing discs, it appears to be required in all cells. Null alleles, which are cell lethal in a *swm*/+ background, share some, but not all characteristics of *Minute* ribosomal protein mutants. Although *swm* mutants do not have thin bristles as is characteristic of *Minutes*, they are recessive lethal and developmentally delayed, and they interact genetically with *Minutes* and *Minute*-like loci (Gay and Contamine 1993). The wings of the *Minute* locus *RpL38* have defects which are similar to *swm* wings—extra venation, expanded distance between veins 3 and 4, wing hair polarity abnormalities, and increased cell size (Marygold *et al.* 2005). Although $RpL38^{45\text{-}72}$, *Df(2R)M41A10*, and $M41^{A4}$ suppressed hh^{Mrt}, they did not interact with *smo RNAi* or *smo5A* (data not shown). We can speculate only on the basis of aspects of the *Minute* phenotype that are shared with Hh signaling.

While the interactions between *swm* and *Minutes*, as well as the similar phenotypes of *swm* and the *RpL38* genes, might indicate a direct role in ribosome function, both Drosophila Swm and one of its two vertebrate homologs (RBM-27) are nuclear (Kavanagh *et al.* 2005). The presence of RRM sequences in Swm and its homologs might suggest a role in RNA binding or metabolism, and the RRM of RBM-27 binds RNA (Birney *et al.* 1993; Burd and Dreyfuss 1994; Kavanagh *et al.* 2005). However, RRMs can have a structural role in protein–protein interactions independent of RNA binding (Fribourg *et al.* 2003), so we cannot determine the molecular function of Swm and its homologs by genetic methods alone. We are intrigued by the fact that the other vertebrate homolog, RBM-26, was identified as se70-2, an autoantigen that is recognized by sera of cutaneous T-cell lymphoma patients and has been used as a diagnostic marker for this tumor (Eichmuller *et al.* 2001; Dummer *et al.* 2004). In addition, the mouse *RBM-26/se70-2* locus was identified as one of four genes deleted in a region required for normal murine skeletal, cartilage, and craniofacial development (Peterson *et al.*

2002). Perhaps the roles of Hh that extend beyond pattern formation to cell cycle regulation, growth control, and cell polarity signify that Hh signal transduction integrates inputs from all three pathways. The pleiotropy of *swm* and *mts* may reflect these multiple inputs.

We thank Susan Younger, Barbara Thomas, Brenda Ng, Li Lin, Frank Hsuing, Gretchen Ehrenkauffer, Brian Biehs, Arjun Guha, Xingwu Lu, Shiho Kawamura, Sougata Roy, Joan Hooper, Chen-Ming Fan, Jeremy Reiter, Chris Wilson, and Pao-Tien Chuang for helpful discussions. For contributing stocks and reagents, we thank the Bloomington Drosophila Stock Center, Ryu Ueda and Kazuko Fujitani (National Institute of Genetics, Mishima, Japan), the Szeged Drosophila Stock Center, Joan Hooper, Wesley Gruber, Yuh-Nun Jan, Suzanne Eaton, Marcel van den Heuvel, Alan Shearn, Michelle Beaucher, Barbara Thomas, Tulle Hazelrigg, Steven Cohen, Fabrice Roegiers, and Bruno Bello. This work was supported by grants from the National Institutes of Health to T.B.K.

LITERATURE CITED

Alcedo, J., Y. Zou and M. Noll, 2000 Posttranscriptional regulation of smoothened is part of a self-correcting mechanism in the Hedgehog signaling system. Mol. Cell **6:** 457–465.

Altschul, S. F., W. Gish, W. Miller, E. W. Myers and D. J. Lipman, 1990 Basic local alignment search tool. J. Mol. Biol. **215:** 403–410.

Apionishev, S., N. M. Katanayeva, S. A. Marks, D. Kalderon and A. Tomlinson, 2005 Drosophila Smoothened phosphorylation sites essential for Hedgehog signal transduction. Nat. Cell Biol. **7:** 86–92.

Apweiler, R., T. K. Attwood, A. Bairoch, A. Bateman, E. Birney *et al.*, 2001 The InterPro database, an integrated documentation resource for protein families, domains and functional sites. Nucleic Acids Res. **29:** 37–40.

Aza-Blanc, P., F. A. Ramirez-Weber, M. P. Laget, C. Schwartz and T. B. Kornberg, 1997 Proteolysis that is inhibited by hedgehog targets Cubitus interruptus protein to the nucleus and converts it to a repressor. Cell **89:** 1043–1053.

Bello, B., H. Reichert and F. Hirth, 2006 The brain tumor gene negatively regulates neural progenitor cell proliferation in the larval central brain of Drosophila. Development **133:** 2639–2648.

Belloni, E., M. Muenke, E. Roessler, G. Traverso, J. Siegel-Bartelt *et al.*, 1996 Identification of Sonic hedgehog as a candidate gene responsible for holoprosencephaly. Nat. Genet. **14:** 353–356.

Birney, E., S. Kumar and A. R. Krainer, 1993 Analysis of the RNA-recognition motif and RS and RGG domains: conservation in metazoan pre-mRNA splicing factors. Nucleic Acids Res. **21:** 5803–5816.

Brand, A. H., and N. Perrimon, 1993 Targeted gene expression as a means of altering cell fates and generating dominant phenotypes. Development **118:** 401–415.

Burd, C. G., and G. Dreyfuss, 1994 Conserved structures and diversity of functions of RNA-binding proteins. Science **265:** 615–621.

Burke, R., D. Nellen, M. Bellotto, E. Hafen, K. A. Senti *et al.*, 1999 Dispatched, a novel sterol-sensing domain protein dedicated to the release of cholesterol-modified hedgehog from signaling cells. Cell **99:** 803–815.

Callejo, A., C. Torroja, L. Quijada and I. Guerrero, 2006 Hedgehog lipid modifications are required for Hedgehog stabilization in the extracellular matrix. Development **133:** 471–483.

Capdevila, J., F. Pariente, J. Sampedro, J. L. Alonso and I. Guerrero, 1994 Subcellular localization of the segment polarity protein patched suggests an interaction with the wingless reception complex in Drosophila embryos. Development **120:** 987–998.

Casso, D. J., S. Tanda, B. Biehs, B. Martoglio and T. B. Kornberg, 2005 Drosophila signal peptide peptidase is an essential protease for larval development. Genetics **170:** 139–148.

Chamoun, Z., R. K. Mann, D. Nellen, D. P. von Kessler, M. Bellotto *et al.*, 2001 Skinny hedgehog, an acyltransferase required for palmitoylation and activity of the hedgehog signal. Science **293:** 2080–2084.

Chen, Y., and G. Struhl, 1996 Dual roles for patched in sequestering and transducing Hedgehog. Cell **87:** 553–563.

Chen, Y., N. Gallaher, R. H. Goodman and S. M. Smolik, 1998 Protein kinase A directly regulates the activity and proteolysis of cubitus interruptus. Proc. Natl. Acad. Sci. USA **95:** 2349–2354.

Chen, M. H., Y. J. Li, T. Kawakami, S. M. Xu and P. T. Chuang, 2004 Palmitoylation is required for the production of a soluble multimeric Hedgehog protein complex and long-range signaling in vertebrates. Genes Dev. **18:** 641–659.

Chiang, C., Y. Litingtung, E. Lee, K. E. Young, J. L. Corden *et al.*, 1996 Cyclopia and defective axial patterning in mice lacking Sonic hedgehog gene function. Nature **383:** 407–413.

Chou, T. B., and N. Perrimon, 1992 Use of a yeast site-specific recombinase to produce female germline chimeras in Drosophila. Genetics **131:** 643–653.

Clyne, P. J., J. S. Brotman, S. T. Sweeney and G. Davis, 2003 Green fluorescent protein tagging Drosophila proteins at their native genomic loci with small P elements. Genetics **165:** 1433–1441.

Cokol, M., R. Nair and B. Rost, 2000 Finding nuclear localization signals. EMBO Rep. **1:** 411–415.

Collins, R. T., and S. M. Cohen, 2005 A genetic screen in Drosophila for identifying novel components of the hedgehog signaling pathway. Genetics **170:** 173–184.

Colosimo, P. F., and N. S. Tolwinski, 2006 Wnt, Hedgehog and junctional Armadillo/beta-catenin establish planar polarity in the Drosophila embryo. PLoS ONE **1:** e9.

Dawber, R. J., S. Hebbes, B. Herpers, F. Docquier and M. van den Heuvel, 2005 Differential range and activity of various forms of the Hedgehog protein. BMC Dev. Biol. **5:** 21.

Denef, N., D. Neubuser, L. Perez and S. M. Cohen, 2000 Hedgehog induces opposite changes in turnover and subcellular localization of patched and smoothened. Cell **102:** 521–531.

Dong, X., K. H. Zavitz, B. J. Thomas, M. Lin, S. Campbell *et al.*, 1997 Control of G1 in the developing Drosophila eye: rca1 regulates Cyclin A. Genes Dev. **11:** 94–105.

Duman-Scheel, M., L. Weng, S. Xin and W. Du, 2002 Hedgehog regulates cell growth and proliferation by inducing Cyclin D and Cyclin E. Nature **417:** 299–304.

Dummer, R., J. C. Hassel, F. Fellenberg, S. Eichmuller, T. Maier *et al.*, 2004 Adenovirus-mediated intralesional interferon-gamma gene transfer induces tumor regressions in cutaneous lymphomas. Blood **104:** 1631–1638.

Eaton, S., 2006 Release and trafficking of lipid-linked morphogens. Curr. Opin. Genet. Dev. **16:** 17–22.

Eichmuller, S., D. Usener, R. Dummer, A. Stein, D. Thiel *et al.*, 2001 Serological detection of cutaneous T-cell lymphoma-associated antigens. Proc. Natl. Acad. Sci. USA **98:** 629–634.

Felsenfeld, A. L., and J. A. Kennison, 1995 Positional signaling by hedgehog in Drosophila imaginal disc development. Development **121:** 1–10.

Feng, J., B. White, O. V. Tyurina, B. Guner, T. Larson *et al.*, 2004 Synergistic and antagonistic roles of the Sonic hedgehog N- and C-terminal lipids. Development **131:** 4357–4370.

Foley, E., and F. Sprenger, 2001 The cyclin-dependent kinase inhibitor Roughex is involved in mitotic exit in Drosophila. Curr. Biol. **11:** 151–160.

Fribourg, S., D. Gatfield, E. Izaurralde and E. Conti, 2003 A novel mode of RBD-protein recognition in the Y14-Mago complex. Nat. Struct. Biol. **10:** 433–439.

Gallet, A., R. Rodriguez, L. Ruel and P. P. Therond, 2003 Cholesterol modification of hedgehog is required for trafficking and movement, revealing an asymmetric cellular response to hedgehog. Dev. Cell **4:** 191–204.

Gallet, A., L. Ruel, L. Staccini-Lavenant and P. P. Therond, 2006 Cholesterol modification is necessary for controlled planar long-range activity of Hedgehog in Drosophila epithelia. Development **133:** 407–418.

Gay, P., and D. Contamine, 1993 Study of the ref(2)P locus of Drosophila melanogaster. II. Genetic studies of the 37DF region. Mol. Gen. Genet. **239:** 361–370.

Gustavson, E., A. S. Goldsborough, Z. Ali and T. B. Kornberg, 1996 The Drosophila *engrailed* and *invected* genes: partners in regulation, expression, and function. Genetics **142:** 893–906.

Haines, N., and M. van den Heuvel, 2000 A directed mutagenesis screen in Drosophila melanogaster reveals new mutants that influence hedgehog signaling. Genetics **156:** 1777–1785.

Hannus, M., F. Feiguin, C. P. Heisenberg and S. Eaton, 2002 Planar cell polarization requires Widerborst, a B′ regulatory subunit of protein phosphatase 2A. Development **129:** 3493–3503.

Hooper, J. E., 1994 Distinct pathways for autocrine and paracrine Wingless signalling in Drosophila embryos. Nature **372:** 461–464.

Hooper, J. E., and M. P. Scott, 2005 Communicating with Hedgehogs. Nat. Rev. Mol. Cell. Biol. **6:** 306–317.

Jia, J., K. Amanai, G. Wang, J. Tang, B. Wang *et al.*, 2002 Shaggy/GSK3 antagonizes Hedgehog signalling by regulating Cubitus interruptus. Nature **416:** 548–552.

Jia, J., C. Tong, B. Wang, L. Luo and J. Jiang, 2004 Hedgehog signalling activity of Smoothened requires phosphorylation by protein kinase A and casein kinase I. Nature **432:** 1045–1050.

Kavanagh, S. J., T. C. Schulz, P. Davey, C. Claudianos, C. Russell *et al.*, 2005 A family of RS domain proteins with novel subcellular localization and trafficking. Nucleic Acids Res. **33:** 1309–1322.

Lawrence, P. A., G. Struhl and J. Casal, 2007 Planar cell polarity: One or two pathways? Nat. Rev. Genet. **8:** 555–563.

Lee, J. D., and J. E. Treisman, 2001 Sightless has homology to transmembrane acyltransferases and is required to generate active Hedgehog protein. Curr. Biol. **11:** 1147–1152.

Lee, T., C. Winter, S. S. Marticke, A. Lee and L. Luo, 2000 Essential roles of Drosophila RhoA in the regulation of neuroblast proliferation and dendritic but not axonal morphogenesis. Neuron **25:** 307–316.

Lee, Y. S., and R. W. Carthew, 2003 Making a better RNAi vector for Drosophila: use of intron spacers. Methods **30:** 322–329.

Liu, Y., X. Cao, J. Jiang and J. Jia, 2007 Fused Costal2 protein complex regulates Hedgehog-induced Smo phosphorylation and cell-surface accumulation. Genes Dev. **21:** 1949–1963.

Lu, X., S. Liu and T. B. Kornberg, 2006 The C-terminal tail of the Hedgehog receptor Patched regulates both localization and turnover. Genes Dev. **20:** 2539–2551.

Lum, L., S. Yao, B. Mozer, A. Rovescalli, D. Von Kessler *et al.*, 2003 Identification of Hedgehog pathway components by RNAi in Drosophila cultured cells. Science **299:** 2039–2045.

Marygold, S. J., C. M. Coelho and S. J. Leevers, 2005 Genetic analysis of *RpL38* and *RpL5*, two minute genes located in the centric heterochromatin of chromosome 2 of *Drosophila melanogaster*. Genetics **169:** 683–695.

Micchelli, C. A., I. The, E. Selva, V. Mogila and N. Perrimon, 2002 Rasp, a putative transmembrane acyltransferase, is required for Hedgehog signaling. Development **129:** 843–851.

Motzny, C. K., and R. Holmgren, 1995 The Drosophila Cubitus interruptus protein and its role in the *wingless* and *hedgehog* signal transduction pathways. Mech. Dev. **52:** 137–150.

Mullor, J. L., M. Calleja, J. Capdevila and I. Guerrero, 1997 Hedgehog activity, independent of decapentaplegic, participates in wing disc patterning. Development **124:** 1227–1237.

Nusslein-Volhard, C., and E. Wieschaus, 1980 Mutations affecting segment number and polarity in Drosophila. Nature **287:** 795–801.

Nybakken, K., S. A. Vokes, T. Y. Lin, A. P. McMahon and N. Perrimon, 2005 A genome-wide RNA interference screen in Drosophila melanogaster cells for new components of the Hh signaling pathway. Nat. Genet. **37:** 1323–1332.

Nybakken, K. E., C. W. Turck, D. J. Robbins and J. M. Bishop, 2002 Hedgehog-stimulated phosphorylation of the kinesin-related protein Costal2 is mediated by the serine/threonine kinase fused. J. Biol. Chem. **277:** 24638–24647.

Ogden, S. K., D. J. Casso, M. Ascano, Jr., M. M. Yore, T. B. Kornberg *et al.*, 2006 Smoothened regulates activator and repressor functions of Hedgehog signaling via two distinct mechanisms. J. Biol. Chem. **281:** 7237–7243.

Pasca di Magliano, M., and M. Hebrok, 2003 Hedgehog signalling in cancer formation and maintenance. Nat. Rev. Cancer **3:** 903–911.

Pepinsky, R. B., C. Zeng, D. Wen, P. Rayhorn, D. P. Baker *et al.*, 1998 Identification of a palmitic acid-modified form of human Sonic hedgehog. J. Biol. Chem. **273:** 14037–14045.

Peterson, K. A., B. L. King, A. Hagge-Greenberg, J. J. Roix, C. J. Bult *et al.*, 2002 Functional and comparative genomic analysis of the piebald deletion region of mouse chromosome 14. Genomics **80:** 172–184.

Porter, J. A., K. E. Young and P. A. Beachy, 1996 Cholesterol modification of hedgehog signaling proteins in animal development. Science **274:** 255–259.

Price, M. A., and D. Kalderon, 2002 Proteolysis of the Hedgehog signaling effector Cubitus interruptus requires phosphorylation by Glycogen Synthase Kinase 3 and Casein Kinase 1. Cell **108:** 823–835.

Quirk, J., M. van den Heuvel, D. Henrique, V. Marigo, T. A. Jones *et al.*, 1997 The smoothened gene and hedgehog signal transduction in Drosophila and vertebrate development. Cold Spring Harbor Symp. Quant. Biol. **62:** 217–226.

Ramirez-Weber, F. A., D. J. Casso, P. Aza-Blanc, T. Tabata and T. B. Kornberg, 2000 Hedgehog signal transduction in the posterior compartment of the Drosophila wing imaginal disc. Mol. Cell **6:** 479–485.

Reardon, J. T., C. A. Liljestrand-Golden, R. L. Dusenbery and P. D. Smith, 1987 Molecular analysis of diepoxybutane-induced mutations at the rosy locus of *Drosophila melanogaster*. Genetics **115:** 323–331.

Roessler, E., E. Belloni, K. Gaudenz, P. Jay, P. Berta *et al.*, 1996 Mutations in the human Sonic Hedgehog gene cause holoprosencephaly. Nat. Genet. **14:** 357–360.

Schier, A. F., S. C. Neuhauss, K. A. Helde, W. S. Talbot and W. Driever, 1997 The one-eyed pinhead gene functions in mesoderm and endoderm formation in zebrafish and interacts with no tail. Development **124:** 327–342.

Snaith, H. A., C. G. Armstrong, Y. Guo, K. Kaiser and P. T. Cohen, 1996 Deficiency of protein phosphatase 2A uncouples the nuclear and centrosome cycles and prevents attachment of microtubules to the kinetochore in Drosophila microtubule star (mts) embryos. J. Cell Sci. **109**(Pt 13): 3001–3012.

Strigini, M., and S. M. Cohen, 1997 A Hedgehog activity gradient contributes to AP axial patterning of the Drosophila wing. Development **124:** 4697–4705.

Tabata, T., and T. B. Kornberg, 1994 Hedgehog is a signaling protein with a key role in patterning Drosophila imaginal discs. Cell **76:** 89–102.

Tabata, T., and Y. Takei, 2004 Morphogens, their identification and regulation. Development **131:** 703–712.

Tabata, T., S. E. Eaton and T. B. Kornberg, 1992 The Drosophila hedgehog gene is expressed specifically in posterior compartment cells and is a target of engrailed regulation. Genes Dev. **6:** 2635–2645.

Tabata, T., C. Schwartz, E. Gustavson, Z. Ali and T. B. Kornberg, 1995 Creating a Drosophila wing de novo, the role of engrailed, and the compartment border hypothesis. Development **121:** 3359–3369.

Uemura, T., K. Shiomi, S. Togashi and M. Takeichi, 1993 Mutation of twins encoding a regulator of protein phosphatase 2A leads to pattern duplication in Drosophila imaginal discs. Genes Dev. **7:** 429–440.

Vegh, M., and K. Basler, 2003 A genetic screen for hedgehog targets involved in the maintenance of the Drosophila anteroposterior compartment boundary. Genetics **163:** 1427–1438.

Wassarman, D. A., N. M. Solomon, H. C. Chang, F. D. Karim, M. Therrien *et al.*, 1996 Protein phosphatase 2A positively and negatively regulates Ras1-mediated photoreceptor development in Drosophila. Genes Dev. **10:** 272–278.

Yao, S., L. Lum and P. Beachy, 2006 The ihog cell-surface proteins bind Hedgehog and mediate pathway activation. Cell **125:** 343–357.

Zecca, M., K. Basler and G. Struhl, 1995 Sequential organizing activities of engrailed, hedgehog and decapentaplegic in the Drosophila wing. Development **8:** 2265–2278.

Zeng, X., J. A. Goetz, L. M. Suber, W. J. Scott, Jr., C. M. Schreiner *et al.*, 2001 A freely diffusible form of Sonic hedgehog mediates long-range signalling. Nature **411:** 716–720.

Zhang, C., E. H. Williams, Y. Guo, L. Lum and P. A. Beachy, 2004 Extensive phosphorylation of Smoothened in Hedgehog pathway activation. Proc. Natl. Acad. Sci. USA **101:** 17900–17907.

Zhang, Y., X. G. Jiang and J. Yao, 2001 Lowering of sodium deoxycholate-induced nasal ciliotoxicity with cyclodextrins. Acta Pharmacol. Sin. **22:** 1045–1050.

Communicating editor: K. V. Anderson